



ELSEVIER

Contents lists available at ScienceDirect

Journal of Luminescence

journal homepage: www.elsevier.com/locate/jlumin

Cerium-, terbium- and europium-activated CaScAlSiO₆ as a full-color emitting phosphor



Wei Lü^{a,*}, Yongchao Jia^{a,b}, Wenzhen Lv^{a,b}, Qi Zhao^{a,b}, Hongpeng You^{a,*}

^a State Key Laboratory of Rare Earth Resource Utilization, Changchun Institute of Applied Chemistry, Chinese Academy of Sciences, Changchun 130022, PR China

^b Graduate University of the Chinese Academy of Sciences, Beijing 100049, PR China

ARTICLE INFO

Article history:

Received 12 July 2013

Received in revised form

17 October 2013

Accepted 1 November 2013

Available online 13 November 2013

Keywords:

Phosphor

Full-color emitting

Fluorescent lamps

ABSTRACT

We reported a single-phased CaScAlSiO₆:Ce³⁺, Tb³⁺, Eu³⁺ as a potential full-color emitting phosphor for the application in fluorescent lamps. The CaScAlSiO₆:Ce³⁺, Tb³⁺, Eu³⁺ phosphor exhibits three bands under 254 nm excitation: one band situated at 380 nm is attributed to the 5d→4f transitions of Ce³⁺ ions, the second band with sharp lines peaked at 542 nm is assigned to the ⁵D₄→⁷F_J transitions of Tb³⁺ ions, the third band in the orange–red region (580–700 nm) is originated from ⁵D₀→⁷F_J transitions of Eu³⁺ ions. The Commission Internationale de l'Éclairage (CIE) chromaticity coordinates (0.30, 0.30) and high color rendering index (CRI=88) can be achieved upon excitation of 254 nm light. It is suggested that CaScAlSiO₆:Ce³⁺, Tb³⁺, Eu³⁺ can serve as a potential single-phased full-color emitting phosphor for phosphor-converted fluorescent lamps.

© 2013 Elsevier B.V. All rights reserved.

1. Introduction

Nowadays, rare earth activated phosphors have been widely utilized in illumination devices [1–3]. Especially, phosphors for fluorescent lamps (FLs) are frequently used and produced in the largest quantity for lighting because of their high efficiency and long lifetime. Although the basics of commercial FLs containing a mixture of triphosphors—the blue-emitting BaMgAl₁₀O₁₇:Eu²⁺ [4], the red-emitting Y₂O₃:Eu³⁺ [5], and the green-emitting LaPO₄:Ce³⁺, Tb³⁺ [6] under UV light at 254 nm were well-established, the development of new phosphors continues because of the importance of phosphor efficiency required for different applications [7–9]. As we known, trivalent Tb and Eu ions, as the promising species that provide optical emission in green and red regions, have been investigated by many groups [10–14]. Take the Eu³⁺ ions for example, in the typical used for fluorescent lamps of Y₂O₃:Eu³⁺ phosphor, it has strong optical absorption in the shortwave UV region of 254 nm and gives an efficient red emission [15]. Despite there were sweeping studies on the above fields including Tb³⁺ and Eu³⁺ single doped phosphor in the past years, single-phase full-color emitting phosphors for FLs application were rarely reported [16].

In this research, we report our recent investigation results on the synthesis and luminescence of a full-color emitting CaScAlSiO₆:Ce³⁺, Tb³⁺, Eu³⁺ phosphor. The CIE chromaticity coordinates

(0.30, 0.30) and high color rendering index (CRI=88) can be achieved upon excitation of 254 nm light.

2. Experimental section

The Ca_{1-x}Sc_{1-y-z}AlSiO₆(CSAS):xCe³⁺, yTb³⁺, zEu³⁺ phosphors were synthesized by a high-temperature solid state reaction. The constituent oxides or carbonates CaCO₃ (99.9%), Sc₂O₃ (99.9%), SiO₂ (99.9%), Al₂O₃ (99.9%), CeO₂ (99.99%), Tb₄O₇ (99.99%) and Eu₂O₃ (99.99%) were employed as the raw materials. In the preparation, the complete burning process was achieved by a two-stage solid-state reaction. The starting materials were mixed together with required molar ratio. A small amount of high-purity CeO₂ and Tb₄O₇ were added into the mixture. The reactants were mixed homogeneously by an agate mortar for 30 min, placed in a crucible with a lid, and then sintered in a tubular furnace at 1400 °C for 4 h in reductive atmosphere (10% H₂+90% N₂ mixed flowing gas). Then, a small amount of high-purity Eu₂O₃ was added into the obtained powder. The obtained powder were mixed homogeneously by an agate mortar for 15 min, placed in a crucible with a lid, and then sintered in a tubular furnace at 1400 °C in air. The structure of sintered samples was identified by powder X-ray diffraction (XRD) analysis (Bruker AXS D8), with graphite monochromatized Cu K α radiation ($\lambda=0.15405$ nm) operating at 40 kV and 40 mA. The measurements of photoluminescence (PL) and photoluminescence excitation (PLE) spectra were performed by using a Hitachi F4500 spectrometer equipped with a 150 W xenon lamp under a working voltage of 700 V. The size and

* Corresponding authors. Tel.: +86 431 8526 2798; fax: +86 431 8569 8041.
E-mail addresses: wlv@ciac.ac.cn (W. Lü), hpyou@ciac.ac.cn (H. You).

morphology of the samples were inspected using a field emission scanning electron microscope equipped with an energy-dispersive spectrometer (EDS) (FE-SEM, S-4800, Hitachi, Japan). The CIE and CRI were calculated by SpectraWin software. The luminescence decay curve was obtained from a Lecroy Wave Runner 6100 digital oscilloscope (1 GHz) using a tunable laser (pulse width=4 ns, gate=50 ns) as the excitation source (Continuum Sunlite OPO). We determined the Ce^{3+} concentrations at 4% which the PL intensities reach their maxima under 330 nm light excitation.

3. Results and discussion

Fig. 1(a) shows the XRD patterns of CSAS:0.04 Ce^{3+} , CSAS:0.04 Tb^{3+} , CSAS:0.04 Eu^{3+} and CSAS:0.04 Ce^{3+} , 0.04 Tb^{3+} , 0.04 Eu^{3+} samples. It is clearly observed that the samples are well coincident with the standard data of CSAS with JCPDS card no 77-0465 except for a small amount of impurities. These weak impurity peaks may be assigned to $\text{Sc}_2\text{Si}_2\text{O}_7$ silicate phase. The intensity of impurity phases is so small that the effect on luminescent properties of rare-earth ions doped CSAS could be neglected. The schematic representation of the structural of CSAS host is illustrated in Fig. 1(b). As shown in Fig. 1(b), Ca^{2+} and Sc^{3+} ions are tightly surrounded with tetrahedral SiO_4 and AlO_4 units, and the oxygen atoms form bridges between tetrahedral SiO_4 and AlO_4 . The CSAS host lattice contains two different cation sites:

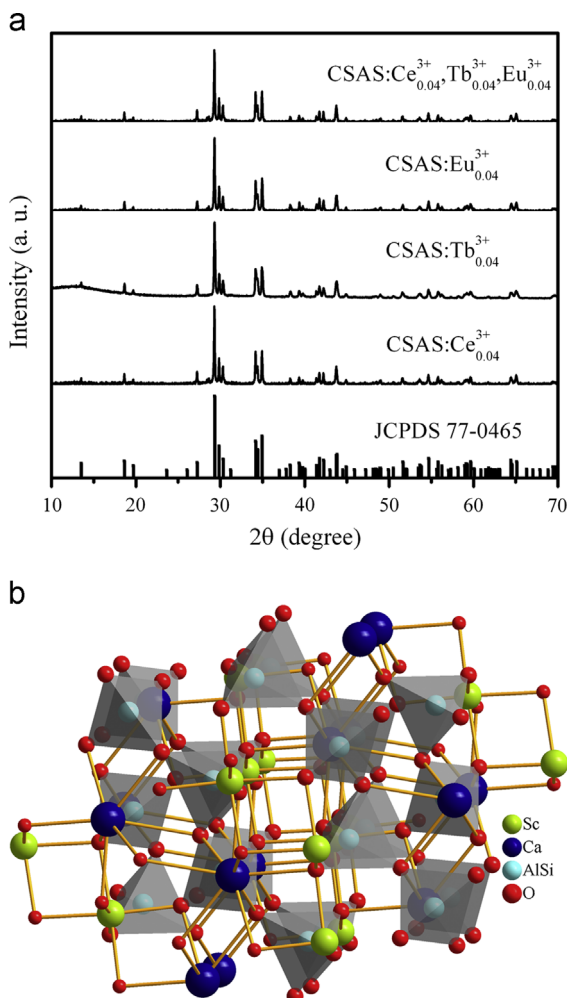


Fig. 1. The XRD patterns of CSAS:0.04 Ce^{3+} , CSAS:0.04 Tb^{3+} , CSAS:0.04 Eu^{3+} and CSAS:0.04 Ce^{3+} , 0.04 Tb^{3+} , 0.04 Eu^{3+} and its schematic view of the structure and coordination environments.

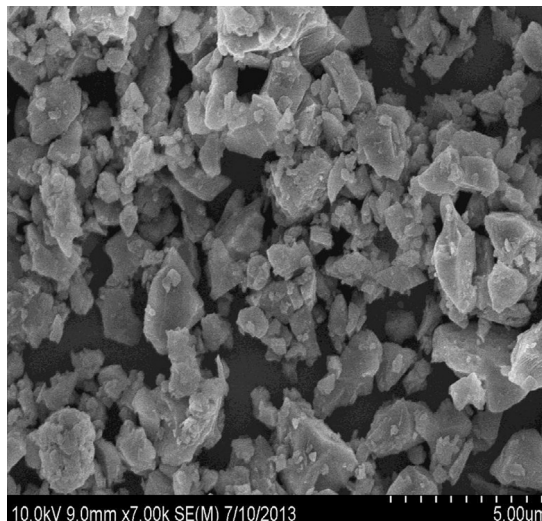


Fig. 2. The typical SEM micrograph of CSAS:0.04 Ce^{3+} , 0.04 Tb^{3+} , 0.04 Eu^{3+} .

8-fold coordinated Ca^{2+} site and 6-fold coordinated Sc^{2+} site. For the consideration of ionic radii matching, it is demonstrated that Ce^{3+} is expected to occupy Ca^{2+} site because the ionic radius of Ce^{3+} (1.14 Å) is close to that of Ca^{2+} (1.12 Å); As for Tb^{3+} (0.92 Å for CN=6, 1.04 Å for CN=8) and Eu^{3+} (0.95 Å for CN=6, 1.07 Å for CN=8), accounting for ion valence, we presume that Tb^{3+} and Eu^{3+} may be favorable to occupy Sc^{3+} (0.75 Å for CN=6, 0.87 Å for CN=8) site. Fig. 2 displays the representative SEM micrograph of CSAS:0.04 Ce^{3+} , 0.04 Tb^{3+} , 0.04 Eu^{3+} . The phosphor powders are uniform and the phosphor crystals show irregular shapes with the dimension of 1–10 μm.

Fig. 3(a) shows the PL and PLE spectra of CSAS:0.04 Ce^{3+} . The PLE spectrum of CSAS: Ce^{3+} consists of three broad bands centered at 245 nm, 296 nm and 340 nm (the strongest), corresponding to the host absorption and 4f–5d transition of Ce^{3+} . While the PL spectrum presents an intense violet light with a peak at 380 nm, which is originated from the 5d→4f transitions of Ce^{3+} ions. The PL and PLE spectra of CSAS:0.04 Tb^{3+} are presented in Fig. 3(b). A charge transfer band (CTB) centered at 233 nm can be found in the range of 200–300 nm, which is attributed to the spin allowed 4f–5d transition of Tb^{3+} ions. The other is composed of a series of weak narrow bands in the 300–500 nm regions, which correspond to absorption f–f transition of Tb^{3+} ions. The Tb^{3+} emission lines are located at 485, 542 nm, 580 nm and 620 nm, which are assigned to the $^5\text{D}_4$ to $^7\text{F}_j$ ($j=6, 5, 4, 3$) multiplet transitions, respectively [17]. In particular, the highest sharp line peaked at 542 nm is characteristic of $^5\text{D}_4$ – $^7\text{F}_5$ of Tb^{3+} 4f–4f transitions. Comparing Fig. 3(a) and (b), it is clearly exhibited that there is a spectral overlap between the Ce^{3+} PL and Tb^{3+} PLE spectra, indicating the possibility of energy transfer from Ce^{3+} to Tb^{3+} in CSAS. Meanwhile, a shortening of the lifetimes of 5d–4f transition of Ce^{3+} with codoping Tb^{3+} ions can be observed, as shown in Fig. 4, which is another proof for the energy transfer from the Ce^{3+} to Tb^{3+} ions [18]. The corresponding energy levels scheme of Ce^{3+} and Tb^{3+} and the possible optical transition involved in the energy transfer processes are schematically depicted in Fig. 5. When Ce^{3+} ions absorb UV light, the excitation energy could be released not only by emitting blue light but also by transferring to Tb^{3+} ions, which finally exhibits a green emission of Tb^{3+} ions. Fig. 3(c) shows the PL and PLE spectra of CSAS:0.04 Eu^{3+} . The PLE spectrum consists of two main features, the abroad band in the range of 200–300 nm is assigned to CTB from O^{2+} to Eu^{3+} [19], and the characteristic f–f transition lines of Eu^{3+} are attributed to the transitions from $^7\text{F}_0$ ground state to the different excited states of Eu^{3+} , with weak peaks at 365 nm ($^3\text{D}_4$), 381 nm ($^5\text{G}_3$) and 391 nm ($^5\text{L}_6$), respectively. The PL spectrum yields multi-emission

Download English Version:

<https://daneshyari.com/en/article/5400040>

Download Persian Version:

<https://daneshyari.com/article/5400040>

[Daneshyari.com](https://daneshyari.com)